Persistent destructive quantum interference in the inverted graph method

M. Niţă
National Institute of Materials Physics, Atomistilor 405A, Magurele 077125, Romania

D. C. Marinescu
Department of Physics, Clemson University, Clemson, South Carolina 29634, USA

(Received 31 January 2022; revised 28 March 2022; accepted 29 March 2022; published 8 April 2022)

We formulate a general criterion that underlies the persistence of conductance zeros induced by destructive quantum interference under the application of external perturbations in physical systems described by a discrete nonsingular Hamiltonian H. Our approach uses nonzero matrix elements of H^{-1} between two lattice points as edges of a graph to indicate the existence of a nonzero conductance between the same points. A given conductance zero, or a missing edge in the *inverted graph*, is preserved when the perturbation, in the form of on-site or additional interpoint hopping energies, is applied only to points outside the set of first-order graph neighbors of either the entry lead or the exit lead. We discuss the application of these results to a study of the robustness of the conductance zeros in the fulvene and benzene molecules.

DOI: 10.1103/PhysRevB.105.155303

I. INTRODUCTION

Understanding the cancellation of the electric conductance on account of destructive quantum interference (DQI) of the electron paths in mesoscopic devices, such as molecules and nanostructures, has been an intense field of study in the past two decades [1–10]. Controlling this quantum phenomenon by means of external parameters can potentially lead to the development of many interesting applications, such as molecular switchers, quantum interference transistors, or thermoelectric devices [11–20].

Previously, it was shown that for some lattice systems the conductance zeros are robust under new external electrode attachment [12], heteroatom substitutions [15,21–24], Büttiker probe addition at some lattice positions [13], the addition of new atom groups at the contact positions [25], or for some external potentials such as single and multisite perturbations in bipartite lattices [26] and beyond these [27]. In bipartite lattices a given conductance zero was found to be invariant under broad conditions. In these systems, which are composed of two sublattices, the destructive interferences realized in transport between the same sublattice points are always zero [28]. Further, they are not modified by any same-sublattice site perturbation [22,26]. A generalization of this property in more complex systems, beyond bipartite lattices, was recently demonstrated in Ref. [27].

In this paper, we further such considerations by developing a general criterion regarding the invariance properties of a given conductance zero in systems described by a nonsingular, discrete Hamiltonian (i.e., H^{-1} exists). To this end we formulate the inverted graph method associated with a discrete Hamiltonian for propagation modes at zero energy. This approach exploits the equality between the Green's function matrix elements between two lattice sites $G_{ij} = [(E - H)^{-1}]_{ij}$ evaluated at $E = 0$ and the matrix elements of $-H^{-1}$ to construct a visual representation of the nonzero conductance paths as edges connecting the vertices of a graph of the lattice sites. The Green's function matrix element proportionality with the measured conductance **G** between the same points used as input and output in the Büttiker formalism [27,29,30] allows a straightforward interpretation of the inverse graph as a conductance map of the system.

The idea to identify the DQI process using the zero entries of the H^{-1} matrix was used in the literature in Refs. [7,31]. There all the zero values obtained for a molecular system where collected in a graph representation whose lines (i, j) indicate the DQI process $G_{ij} = 0$ (as described in Fig. 1 in Ref. [31] for benzene and Scheme 18 in Ref. [7] for annulene). Here we adopt an opposite picture, where we interpret as edges in a graph the lines (i, j) that correspond to $G_{ij} \neq 0$, while the absence of a line denotes a conductance zero. This inverted graph picture appears to be very useful if one studies general invariance properties of the conductance zeros.

The gist of our theory is discussed in Sec. II where we introduce the model and present the general proof regarding the invariance properties of an arbitrary conductance cancellation. Several ways of lifting this zero are also analyzed. We illustrate the application of the graphical method to a nonbipartite molecule and to a bipartite one in Sec. III, while in Sec. IV we analyze its extension to the $E \neq 0$ case. The conclusions are presented in Sec. V.

II. MODEL AND DEFINITIONS

As a representation of a physical system of interest, we consider the set of lattice points $M = \{n | n = 1, \ldots, \mathcal{N}\}$, which also designates the quantum states of the system $\{|n\rangle\}$. The electron dynamics is dictated by the noninteracting,

discrete Hamiltonian:

$$H = \sum_{n,m\in \mathrm{M}} h_{n,m}|n\rangle\langle m|, \tag{1}$$

whose matrix representation has elements equal to $h_{n,m} = \langle n|H|m\rangle$. These are hopping or on-site energies of the discrete model for $n \neq m$ or $n = m$, respectively. The Hamiltonian matrices discussed in the paper are nonsingular; i.e., they admit an inverse.

A destructive quantum interference process at energy E appears when the probability of the electron propagation between two lattice sites $i, j \in M$ is zero. Physically this occurs when the interference result of the various electron paths in the atomic or orbital space is zero [10]. Mathematically, this is expressed as the cancellation of the matrix element of the Green's function operator, $G(E) = \frac{1}{E-H}$, evaluated between quantum states $|i\rangle$ and $|j\rangle$,

$$G_{ij}(E) = 0. \tag{2}$$

On account of the direct relationship between the Green's function and transport conductance, obtained either in the frame of the Landauer-Büttiker formalism [29,32,33] or in the source and sink potential description [7,34], when two external transport leads (or electrodes) are connected at the sites i and j, the DQI also manifests as an electric conductance zero,

$$\mathbf{G}_{ij}(E) = 0, \tag{3}$$

where energy E is the Fermi energy of the electron propagating through the attached leads [35]. Our study is focused on DQI processes at $E = 0$, a regime analyzed in several other works [7,28]. Henceforth this is not explicitly declared. A short analysis of an $E \neq 0$ case is discussed in Sec. IV.

The existence of DQI, as expressed in Eq. (2), can be deduced in general by various theoretical methods that have already been developed in the literature [2,3,7,26–28,31,36]. Here, however, we formulate a general algorithm for predicting the robustness features of a given conductance zero when additional perturbations are added to the system.

Since H is nonsingular, the inverse of its matrix H^{-1} exists and can be calculated analytically or numerically. Using the nonzero matrix elements of H^{-1} we built the associated inverted graph, a generic example of which is presented in Fig. 1. Vertices or nodes are designed by circles and they represent the lattice points from the set M. The graph edges or lines (i, j) with $i, j \in M$, drawn with solid lines between nodes, correspond to nonzero values of the matrix elements $(H^{-1})_{ij}$. Since $(H^{-1})_{ij} = -G_{ij}(0)$ the graph lines represent nonzero values of the Green's functions at $E = 0$. Considering the relation between Green's function zeros and conductance zeros discussed above, the lines (i, j) of the inverted graph give the nonzero values of the electrical conductance $\mathbf{G}_{ij} \neq 0$. The absence of a line between two points i and j in Fig. 1 indicates the existence of a conductance zero $\mathbf{G}_{ij} = 0$ that is realized as a result of a destructive DQI process.

To every point $i_0 \in M$ one can associate two disjoint sets of points. One is the neighbor set N_{i_0} that contains the nearest points of i_0, i.e., all adjacent vertexes in the graph [37]. This means that there is a graph line (n, i_0) between any point $n \in N_{i_0}$ and the point i_0, or equivalently a nonzero Green's function

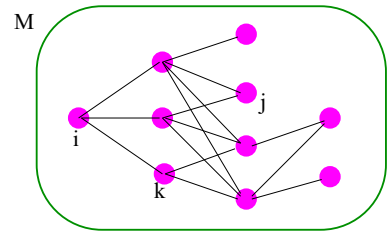

FIG. 1. A schematic representation of the inverse matrix of a nonsingular discrete Hamiltonian H, which designates the inverted graph H^{-1}. The graph vertices are the points $1, \ldots, \mathcal{N}$ from the set M. A graph line (i, k) indicates $(H^{-1})_{ik} = -G_{ik}(0) \neq 0$, while its absence indicates the existence of the DQI process $(H^{-1})_{ij} = -G_{ij}(0) = 0$.

matrix element:

$$N_{i_0} = \{n \in M | G_{ni_0}(0) \neq 0\}. \tag{4}$$

All the sites that do not belong to N_{i_0} form the non-neighbor set $N_{i_0}^{\perp} = M \setminus N_{i_0}$. No lines can be drawn between the points in $N_{i_0}^{\perp}$ and i_0. Correspondingly, this situation is associated with a zero in the Green's function matrix element,

$$N_{i_0}^{\perp} = \{n \in M | G_{ni_0}(0) = 0\}. \tag{5}$$

In Fig. 2 the neighbor set of a given point i_0, N_{i_0}, is marked with black circles, connected with the point i_0 by graph edges. The non-neighbor set, $N_{i_0}^{\perp}$, is represented by red circles that have no edge connection with the point i_0.

A. The invariance of the conductance zeros

To study the invariance of the conductance zeros, we consider a general transformation defined by

$$\tilde{H} = H + \sum_{n,m\in M_{\mathrm{inv}}} w_{nm}|n\rangle\langle m|. \tag{6}$$

M_{inv} is a subset of the lattice points M perturbed by the presence of hopping or on-site new energies, w_{nm}. The modified Hamiltonian $\tilde{H}$ can be used to describe heteroatom substitutions [8,15,21–23], the application of an external voltage [11], the attachment of new external leads [12], or to simulate Büttiker probes [13]. The new energy additions induce structural changes of the molecule, one relevant example

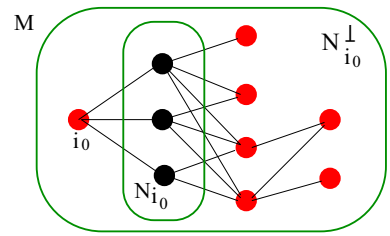

FIG. 2. The two neighborhood sets of an arbitrary point $i_0 \in M$. N_{i_0} is the neighbor set containing the adjacent points of i_0 and is represented by black circles. $N_{i_0}^{\perp}$ is the non-neighbor set containing the remaining points of M, drawn with red circles.

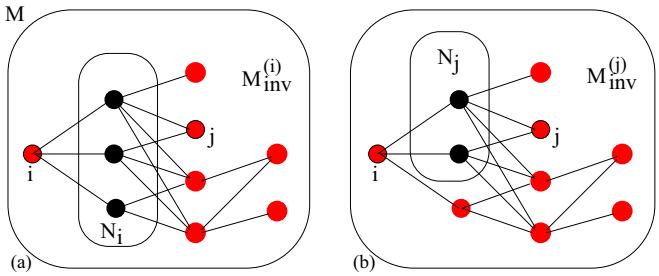

FIG. 3. The two invariance sets, $M_{\text{inv}}^{(i)}$ in panel (a) and $M_{\text{inv}}^{(j)}$ in panel (b), corresponding to a DQI process $\mathbf{G}_{ij} = 0$ are drawn with red circles. Perturbations applied to any of these sets invariably keep the conductance zero.

being the generation of the bicyclic compounds from the original annulene [7].

The transformation in Eq. (6) leaves invariant a given conductance zero between any two points if the newly obtained Green's function defined for $\tilde{H}$ for the same points remains zero. This implies that if Eqs. (2) and (3) occur, after performing the above transformation (6) we obtain

$$\tilde{G}_{ij}(E) = 0. \tag{7}$$

In this case the set M_{inv} is called the invariance set of $G_{ij}(E)$.

A proof of this statement starts by showing that the Green's function zero is unchanged under the application of the perturbation $\tilde{H}$ in Eq. (6) when M_{inv} is identical with the non-neighbor set of i point $N_i^{\perp}$. The Dyson equation written for $\tilde{G}$, $\tilde{G} = G + GW\tilde{G}$, generates

$$\tilde{G}_{ij} = G_{ij} + \sum_{n,m\in N_i^{\perp}} G_{in} w_{nm} \tilde{G}_{mj}. \tag{8}$$

Here, the matrix of the perturbation Hamiltonian W may have nonzero matrix elements w_{nm} only for points $m, n \in N_i^{\perp}$. Thus, for $n \in N_i^{\perp}$, $G_{ni} = G_{in} = 0$ from definition (5). Introducing this in Eq. (8) and using Eq. (2) one obtains the cancellation $\tilde{G}_{ij} = 0$ required in Eq. (7).

Similarly, if we introduce $N_j^{\perp}$, associated with the point j, that leaves the G_{ij} zero unaffected.

The invariance of the Green's function zero is transferred to the related conductance cancellation via the Landauer-Büttiker ansatz [27]. We conclude, therefore, that a certain conductance zero, $\mathbf{G}_{ij} = 0$, persists under a perturbation $\tilde{H}$ that involves lattice sites in either of the two sets,

$$M_{\text{inv}}^{(i)} = N_i^{\perp} \text{ or} \tag{9}$$

$$M_{\text{inv}}^{(j)} = N_j^{\perp}. \tag{10}$$

From definitions in Eqs. (4) and (5) the two invariance sets contain all the vertexes outside the neighbor sets, $M_{\text{inv}}^{(i)} = M - N_i$ and $M_{\text{inv}}^{(j)} = M - N_j$. In Figs. 3(a) and 3(b) they are drawn with the red circles.

In general, the neighbor sets N_i and N_j, and consequently the invariance sets $M_{\text{inv}}^{(i)}$ and $M_{\text{inv}}^{(j)}$, can be disjoint, partially disjoint, equal to each other, or one a subset of the other, as in the generic example of Fig. 3.

The transformations determined by Eq. (6) with M_{inv} in Eqs. (9) and (10) can be used to identify the invariance properties of a given conductance zero as we shown in the examples in Sec. III. If applied to bipartite lattices they recover the invariance properties previously obtained in Refs. [22,26].

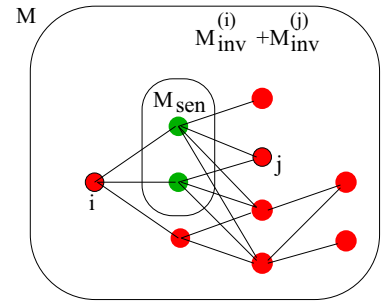

FIG. 4. The sensitiviy set M_{sen} of the conductance $\mathbf{G}_{ij} = 0$.

B. Sensitivity

In this section we show that any single-site perturbation applied outside the invariance sets previously identified, Eqs. (9) and (10), removes the conductance zero. We define the sensitivity set as

$$M_{\text{sen}} = M - M_{\text{inv}}^{(i)} - M_{\text{inv}}^{(j)}, \tag{11}$$

and we show that an additional Hamiltonian perturbation,

$$\tilde{H}' = H + w_n |n\rangle\langle n|, \text{ with } n \in M_{\text{sen}}, \tag{12}$$

will induce a nonzero conductance:

$$\mathbf{G}_{ij} \neq 0. \tag{13}$$

With input from Eqs. (9) and (10) in Eq. (11), the sensitivity set is thus

$$M_{\text{sen}} = N_i \cap N_j, \tag{14}$$

and it contains all the points n for which both G_{ni} and G_{nj} are nonzero, represented in green in Fig. 4.

Previously Ref. [22] established that, in the weak-coupling limit, the addition of an on-site perturbation w_n with simultaneous nonzero matrix elements G_{ni} and G_{nj} affects the G_{ij} matrix element leading to nonzero transport. Here we generalize this result to any coupling constants by writing the Dyson equations for

$$\tilde{G}'_{ij} = G_{ij} + G_{in} w_n \tilde{G}'_{nj}$$

and

$$\tilde{G}'_{nj} = G_{nj} + G_{nn} w_n \tilde{G}'_{nj}.$$

As $G_{ij} = 0$ from our initial choice in Eq. (2), one obtains

$$\tilde{G}'_{ij} = G_{in} \frac{w_n}{1 - w_n G_{nn}} G_{nj}. \tag{15}$$

As stated above, the Green's function $G_{in} \neq 0$ because $n \in N_i$ [see Eqs. (4), (12), and (14)], and $G_{nj} \neq 0$ because n is also in N_j. So in Eq. (15) one has $\tilde{G}'_{ij} \neq 0$ as long as $w_n \neq 0$. By using the effective Hamiltonian formalism [27,35] this leads to a nonzero conductance in Eq. (13) for every coupling of the

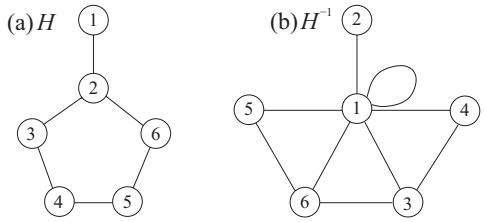

FIG. 5. The fulvene molecule: the direct graph in panel (a) and the inverted graph in panel (b).

transport leads. This result is independent of the value of w_n, which can be real for a heteroatom substitution [22,24] or can be complex when a third lead is attached [12].

III. EXAMPLES

In this section we apply the conclusions previously established to two different molecular systems, one non-bipartite, fulvene, and one bipartite, benzene.

A. Fulvene

The fulvene lattice, pictured in Fig. 5(a), is described by Eq. (1) with the set of points $M = \{1, \ldots, 6\}$. The hopping energies $h_{n,m}$ are nonzero only for the edges of the H graph [solid lines in the Fig. 5(a)] and they all are equal to the energy unit. The inverse matrix of H is numerically calculated and its graph representation is shown in Fig. 5(b) where the edges (n, m) correspond to nonzero matrix elements $(H^{-1})_{nm}$.

Previously it was found that $\mathbf{G}_{45}$ represents a conductance zero of fulvene [27]. Here we investigate its robustness properties. In Fig. 5(b) there is no graph edge between the points 4 and 5, so indeed one has $\mathbf{G}_{45} = 0$. From the graph inspection, the neighbor sets of the contact points 4 and 5 are

$$N_4 = \{1, 3\} \quad \text{and} \tag{16}$$

$$N_5 = \{1, 6\}, \tag{17}$$

and the non-neighbor sets are

$$N_4^{\perp} = \{2, 4, 5, 6\} \text{ and} \tag{18}$$

$$N_5^{\perp} = \{2, 3, 4, 5\}. \tag{19}$$

According to Eqs. (9) and (10) the conductance $\mathbf{G}_{45}$ has two invariance sets given by the non-neighbor sets $N_4^{\perp}$ and $N_5^{\perp}$. From Eqs. (18) and (19) one obtains that

$$\mathbf{G}_{45} = 0 \text{ has } \begin{cases} M_{\text{inv}}^{(4)} = \{2, 4, 5, 6\} & \text{and} \\ M_{\text{inv}}^{(5)} = \{2, 3, 4, 5\}. \end{cases} \tag{20}$$

It means that any multisite perturbation, including on-site energies, hopping energies, or new external leads, concerning the states indexed by the set $M_{\text{inv}}^{(4)}$ (or $M_{\text{inv}}^{(5)}$), invariably keep the $\mathbf{G}_{45}$ zero.

From Eq. (14) the conductance $\mathbf{G}_{45} = 0$ has the sensitivity set $N_4 \cap N_5$. By using Eqs. (16) and (17) one obtains that

$$\mathbf{G}_{45} = 0 \text{ has } M_{\text{sen}} = \{1\}. \tag{21}$$

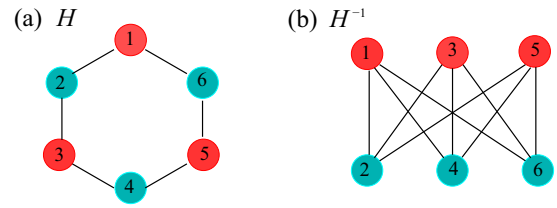

FIG. 6. The benzene molecule: the direct graph in panel (a) and the inverted graph in panel (b).

It means that the conductance $\mathbf{G}_{45}$ becomes nonzero for $w_1 \neq 0$.

In Ref. [27] the invariance sets of the fulvene conductance zeros were studied using the interference points method. In the inverted graph approach the two invariance sets containing the maximum number of possible sites are immediately obtained and they are uniquely defined. When applicable, the method described in Ref. [27] can lead, in principle, to the determination of any number of invariance sets. In this paper, however, we show that they can be reduced to a maximum of 2. Moreover the invariance sets thus calculated are not limited to the quasi-tripartite systems discussed in Ref. [27], since they have been shown to be a general property of any DQI process.

B. Benzene

The inverted graph method can be easily applied to a bipartite molecule, such as meta-contacted benzene, the standard example in this field [2,3,5,10,12,38–40].

Benzene has a hexagonal molecule described by

$$H = \sum_{n,n+1} h_{n,n+1} |n\rangle\langle n+1| + \text{H.c.}, \tag{22}$$

with $n = 1, \ldots, 6$ and $|6 + 1\rangle = |1\rangle$. The set of all points of the benzene lattice is $M = \{1, \ldots, 6\}$, with bipartite subsets $A = \{1, 3, 5\}$ and $B = \{2, 4, 6\}$. The direct graph is pictured in Fig. 6(a). The inverted graph is designed using the values of the H^{-1} matrix elements calculated in Ref. [41] for general cyclic chains. In Fig. 6(b) the benzene has a full bipartite inverted graph as G_{AA} and G_{BB} Green's functions are zero, while all G_{AB} Green's functions are nonzero.

As an example we analyze the robustness properties of $\mathbf{G}_{13}$, a $\mathbf{G}_{AA}$ type conductance. From the inverted graph the neighbor sets of the contact points 1 and 3 are equal to each other:

$$N_1 = N_3 = \{2, 4, 6\}. \tag{23}$$

The non-neighbor sets are

$$N_1^{\perp} = N_3^{\perp} = \{1, 3, 5\}. \tag{24}$$

Introducing Eq. (24) in Eqs. (9) and (10) one obtains that the two invariance sets $M_{\text{inv}}^{(1)}$ and $M_{\text{inv}}^{(3)}$ are equal to each other, and therefore, the meta-contacted conductance

$$\mathbf{G}_{13} = 0 \text{ has } M_{\text{inv}} = \{1, 3, 5\}. \tag{25}$$

Consequently, any combination of on-site and hopping energies w_1, w_3, w_5, w_{13}, w_{31}, w_{15}, w_{51}, w_{35}, and w_{53} maintains the zero values of transport.

What remains outside the invariance set in Eq. (25) is the set of points whose perturbation destroys the given $\mathbf{G}_{13}$ zero.

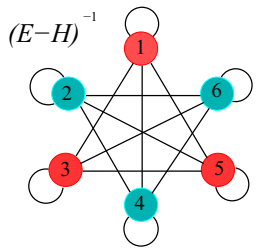

FIG. 7. The inverted graph at $E = \sqrt{2}$ for the benzene molecule.

The sensitivity set is derived from Eqs. (14) and (23). One obtains that

$$\mathbf{G}_{13} = 0 \text{ has } M_{\text{sen}} = \{2, 4, 6\}, \tag{26}$$

which contains the B points of the lattice. The $\mathbf{G}_{13}$ becomes nonzero for $w_2 \neq 0$, $w_4 \neq 0$, or $w_6 \neq 0$. This perturbations may include external leads attached at the B lattice points as was proposed for the quantum interference transistor in Ref. [12], new added atoms as in Refs. [42,43], or atomically precise gating as done in Ref. [44].

The results obtained for benzene are applicable to any $4K + 2$ circular molecule. Based on the $E = 0$ Green's functions calculated in Ref. [41] they have a fully bipartite inverted graph as in Fig. 6(b).

IV. THE $E \neq 0$ CASE

The algorithm presented here is valid for all instances when the Green's function and the conductance cancel, even if the cancellation does not happen at $E = 0$. The difference is that in this case the inverted graph is the lattice representation of $(E - H)^{-1}$. One such example is the DQI process for the ortho configuration in a benzene molecule at $E = \pm\sqrt{2}$ [6], when one has

$$\mathbf{G}_{12}(\sqrt{2}) = 0. \tag{27}$$

To determine the robustness properties of this zero, we calculate the inverse matrix $(\sqrt{2} - H)^{-1}$ with H from Eq. (22). The presence of a line (i, j) in the graph of Fig. 7 means that $G_{ij}(\sqrt{2}) \neq 0$ and the absence means the opposite, that $G_{ij}(\sqrt{2}) = 0$.

From Fig. 7 one determines the neighbor sets of 1 and 2:

$$N_1 = \{1, 3, 4, 5\} \text{ and} \tag{28}$$

$$N_2 = \{2, 4, 5, 6\}. \tag{29}$$

By using the formula of the two invariance sets from Eqs. (9) and (10) and calculating the non-neighbor sets as $M - N_1$ and $M - N_2$, one obtains that

$$\mathbf{G}_{12}(\sqrt{2}) = 0 \text{ has } \begin{cases} M_{\text{inv}}^{(1)} = \{2, 6\} & \text{and} \\ M_{\text{inv}}^{(2)} = \{1, 3\}. \end{cases} \tag{30}$$

It means, for instance, that any multisite perturbations of the sites 2 and 6 (or sites 1 and 3) preserve the conductance zero from Eq. (27).

Introducing Eqs. (28) and (29) in Eq. (14) one obtains that

$$\mathbf{G}_{12}(\sqrt{2}) = 0 \text{ has } M_{\text{sen}} = \{4, 5\}. \tag{31}$$

This result indicates that if one wants to lift up the ortho-contacted conductance from Eq. (27) a single site perturbation $w_4 \neq 0$ or $w_5 \neq 0$ can be used.

V. CONCLUSIONS

In this paper we discuss the general robustness features of the conductance cancellations in quantum systems described by a discrete nonsingular Hamiltonian H. A graphic method which permits the direct visualization of the nonzero conductance paths between two lattice points is introduced to analyze the effect of additional perturbation of a given conductance zero.

It is found that any $\mathbf{G}_{ij} = 0$ conductance cancellation is invariant under external perturbations, be those on-site or hopping energies, applied to lattice points that belong to the two invariance sets called $M_{\text{inv}}^{(i)}$ or $M_{\text{inv}}^{(j)}$. By using the topological features of the inverted graph, these are found to be the non-neighbor sets of the lead contact points i and j, respectively. Moreover, we showed that any single-site perturbation acting on a site outside the reunion of the invariance sets leads to a nonzero output of transport.

Beyond the theoretical interest, knowing the way to fully control the conductance cancellations in molecules and physical lattices, as shown in this paper, helps in further developments of the reliable devices based on the quantum interference phenomena.

ACKNOWLEDGMENTS

The work is supported by Romanian Core Program PN19-03 (Contract No. 21 N/08. 02. 2019).

[1] H.-W. Lee, Generic Transmission Zeros and In-Phase Resonances in Time-Reversal Symmetric Single Channel Transport, Phys. Rev. Lett. **82**, 2358 (1999).

[2] P. W. Fowler, B. T. Pickup, T. Z. Todorova, and W. Myrvold, A selection rule for molecular conduction, J. Chem. Phys. **131**, 044104 (2009).

[3] T. Markussen, R. Stadler, and K. S. Thygesen, The relation between structure and quantum interference in single molecule junctions, Nano Lett. **10**, 4260 (2010).

[4] K. G. L. Pedersen, M. Strange, M. Leijnse, P. Hedegård, G. C. Solomon, and J. Paaske, Quantum interference in off-resonant transport through single molecules, Phys. Rev. B **90**, 125413 (2014).

[5] R. Sýkora and T. Novotný, Comment on "Is the antiresonance in meta-contacted benzene due to the destructive superposition of waves traveling two different routes around the benzene ring", J. Phys. Chem. C **121**, 19538 (2017).

[6] P. Sam-ang and M. G. Reuter, Characterizing destructive quantum interference in electron transport, New J. Phys. **19**, 053002 (2017).

[7] Y. Tsuji, E. Estrada, R. Movassagh, and R. Hoffmann, Quantum interference, graphs, walks, and polynomials, Chem. Rev. **118**, 4887 (2018).

[8] Z. Y. Mijbil, Quantum interference independence of the heteroatom position, Chem. Phys. Lett. **716**, 69 (2019).

[9] A. Valli, A. Amaricci, V. Brosco, and M. Capone, Interplay between destructive quantum interference and symmetry-breaking phenomena in graphene quantum junctions, Phys. Rev. B **100**, 075118 (2019).

[10] S. Gunasekaran, J. E. Greenwald, and L. Venkataraman, Visualizing quantum interference in molecular junctions, Nano Lett. **20**, 2843 (2020).

[11] R. Baer and D. Neuhauser, Anti-coherence based molecular electronics: XOR-gate response, Chem. Phys. **281**, 353 (2002).

[12] D. M. Cardamone, C. A. Stafford, and S. Mazumdar, Controlling quantum transport through a single molecule, Nano Lett. **6**, 2422 (2006).

[13] S. Chen, G. Chen, and M. A. Ratner, Designing principles of molecular quantum interference effect transistors, J. Phys. Chem. Lett. **9**, 2843 (2018).

[14] Z.-Z. Li and M. Leijnse, Quantum interference in transport through almost symmetric double quantum dots, Phys. Rev. B **99**, 125406 (2019).

[15] J. Liu, X. Huang, F. Wang, and W. Hong, Quantum interference effects in charge transport through single-molecule junctions: Detection, manipulation, and application, Acc. Chem. Res. **52**, 151 (2019).

[16] L. J. O'Driscoll and M. R. Bryce, Extended curly arrow rules to rationalise and predict structural effects on quantum interference in molecular junctions, Nanoscale **13**, 1103 (2021).

[17] L. J. O'Driscoll, S. Sangtarash, W. Xu, A. Daaoub, W. Hong, H. Sadeghi, and M. R. Bryce, Heteroatom effects on quantum interference in molecular junctions: Modulating antiresonances by molecular design, J. Phys. Chem. C **125**, 17385 (2021).

[18] R. Miao, H. Xu, M. Skripnik, L. Cui, K. Wang, K. G. L. Pedersen, M. Leijnse, F. Pauly, K. Wärnmark, E. Meyhofer, P. Reddy, and H. Linke, Influence of quantum interference on the thermoelectric properties of molecular junctions, Nano Lett. **18**, 5666 (2018).

[19] X. Wang, T. L. R. Bennett, A. Ismael, L. A. Wilkinson, J. Hamill, A. J. P. White, I. M. Grace, O. V. Kolosov, T. Albrecht, B. J. Robinson, N. J. Long, L. F. Cohen, and C. J. Lambert, Scale-up of room-temperature constructive quantum interference from single molecules to self-assembled molecular-electronic films, J. Am. Chem. Soc. **142**, 8555 (2020).

[20] L. Ma, L.-L. Nian, and J.-T. Lü, Design and optimization of a heat engine based on a porphyrin single-molecule junction with graphene electrodes, Phys. Rev. B **101**, 045410 (2020).

[21] M. H. Garner, G. C. Solomon, and M. Strange, Tunning conductance in aromatic molecules: Constructive and counteractive substituent effects, J. Phys. Chem. C **120**, 9097 (2016).

[22] S. Sangtarash, H. Sadeghi, and C. J. Lambert, Exploring quantum interference in heteroatom-substituted graphene-like molecules, Nanoscale **8**, 13199 (2016).

[23] X. Liu, S. Sangtarash, D. Reber, D. Zhang, H. Sadeghi, J. Shi, Z.-Y. Xiao, W. Hong, C. J. Lambert, and S.-X. Liu, Gating of quantum interference in molecular junctions by heteroatom substitution, Angew. Chem., Int. Ed. **56**, 173 (2017).

[24] S. Sangtarash, H. Sadeghi, and C. J. Lambert, Connectivity-driven bi-thermoelectricity in heteroatom-substituted molecular junctions, Phys. Chem. Chem. Phys. **20**, 9630 (2018).

[25] Y. Tsuji, T. Stuyver, S. Gunasekaran, and L. Venkataraman, The influence of linkers on quantum interference: A linker theorem, J. Phys. Chem. C **121**, 14451 (2017).

[26] M. Niţă, M. Ţolea, and D. C. Marinescu, Robust conductance zeros in graphene quantum dots and other bipartite systems, Phys. Rev. B **101**, 235318 (2020).

[27] M. Niţă, M. Ţolea, and D. C. Marinescu, Conductance zeros in complex molecules and lattices from the interference set method, Phys. Rev. B **103**, 125307 (2021).

[28] F. Evers, R. Korytár, S. Tewari, and J. M. van Ruitenbeek, Advances and challenges in single-molecule electron transport, Rev. Mod. Phys. **92**, 035001 (2020).

[29] M. Büttiker, Four-Terminal Phase-Coherent Conductance, Phys. Rev. Lett. **57**, 1761 (1986).

[30] B. Ostahie, M. Niţă, and A. Aldea, Non-Hermitian approach of edge states and quantum transport in a magnetic field, Phys. Rev. B **94**, 195431 (2016).

[31] R. Sýkora and T. Novotný, Graph-theoretical evaluation of the inelastic propensity rules for molecules with destructive quantum interference, J. Chem. Phys. **146**, 174114 (2017).

[32] R. Landauer, Spatial variation of currents and fields due to localized scatterers in metallic conduction, IBM J. Res. Dev. **1**, 223 (1957).

[33] Y. Imry and R. Landauer, Conductance viewed as transmission, Rev. Mod. Phys. **71**, S306 (1999).

[34] F. Goyer, M. Ernzerhof, and M. Zhuang, Source and sink potentials for the description of open systems with a stationary current passing through, J. Chem. Phys. **126**, 144104 (2007).

[35] M. Ţolea, M. Niţă, and A. Aldea, Analyzing the measured phase in the multichannel Aharonov-Bohm interferometer, Physica E (Amsterdam, Neth.) **42**, 2231 (2010).

[36] A. Levy Yeyati and M. Büttiker, Scattering phases in quantum dots: An analysis based on lattice models, Phys. Rev. B **62**, 7307 (2000).

[37] J. W. Essam, Some basic definitions in graph theory, Rev. Mod. Phys. **42**, 272 (1970).

[38] P. Sautet and C. Joachim, Electronic interference produced by a benzene embedded in a polyacetylene chain, Chem. Phys. Lett. **153**, 511 (1988).

[39] D. Nozaki and C. Toher, Is the antiresonance in meta-contacted benzene due to the destructive superposition of waves traveling two different routes around the benzene ring? J. Phys. Chem. C **121**, 11739 (2017).

[40] D. Nozaki and C. Toher, Reply to Comment on "Is the antiresonance in meta-contacted benzene due to the destructive superposition of waves traveling two different routes around the benzene ring?" J. Phys. Chem. C **121**, 19540 (2017).

[41] R. Movassagh, G. Strang, Y. Tsuji, and R. Hoffmann, The Green's function for the Hückel (tight binding) model, J. Math. Phys. **58**, 033505 (2017).

[42] F. Jiang, D. I. Trupp, N. Algethami, H. Zheng, W. He, A. Alqorashi, C. Zhu, C. Tang, R. Li, H. Sadeghi, J. Shi, R. Davidsson, M. Korb, A. N. Sobolev, M. Naher, S. Sangtarash, P. J. Low, W. Hong, and C. J. Lambert, Turning the tap: Conformational control of quantum interference to modulate

single molecule conductance, Angew. Chem., Int. Ed. **58**, 18987 (2019).

[43] L. A. Zotti and E. Leary, Taming quantum interference in single molecule junctions: Induction and resonance are key, Phys. Chem. Chem. Phys. **22**, 5638 (2020).

[44] C. Tang, L. Huang, S. Sangtarash, M. Noori, H. Sadeghi, H. Xia, and W. Hong, Reversible switching between destructive and constructive quantum interference using atomically precise chemical gating of single-molecule junctions, J. Am. Chem. Soc. **143**, 9385 (2021).